Cell, Vol. 89, 263–273, April 18, 1997, Copyright ©1997 by Cell Press

Core Structure of gp41 from the HIV Envelope Glycoprotein

David C. Chan,*† Deborah Fass,*† James M. Berger,* and Peter S. Kim*†
*Whitehead Institute for Biomedical Research
Cambridge, Massachusetts 02142
†Howard Hughes Medical Institute
Department of Biology
Massachusetts Institute of Technology
Cambridge, Massachusetts 02142

Summary

The envelope glycoprotein of human immunodeficiency virus type 1 (HIV-1) consists of a complex of gp120 and gp41. gp120 determines viral tropism by binding to target-cell receptors, while gp41 mediates fusion between viral and cellular membranes. Previous studies identified an α-helical domain within gp41 composed of a trimer of two interacting peptides. The crystal structure of this complex, composed of the peptides N36 and C34, is a six-helical bundle. Three N36 helices form an interior, parallel coiled-coil trimer, while three C34 helices pack in an oblique, antiparallel manner into highly conserved, hydrophobic grooves on the surface of this trimer. This structure shows striking similarity to the low-pH-induced conformation of influenza hemagglutinin and likely represents the core of fusion-active gp41. Avenues for the design/discovery of small-molecule inhibitors of HIV infection are directly suggested by this structure.

Introduction

The surface glycoproteins of enveloped viruses play critical roles in the initial events of viral infection, mediating virion attachment to cells and fusion of the viral and cellular membranes. Envelope glycoproteins are also major targets for the anti-viral immune response in infected hosts. The human immunodeficiency virus type 1 (HIV-1) envelope glycoprotein consists of two noncovalently associated subunits, gp120 and gp41, that are generated by proteolytic cleavage of a precursor polypeptide, gp160 (review, Luciw, 1996; Freed and Martin, 1995). gp120 directs target-cell recognition and viral tropism through interaction with the cell-surface receptor CD4 and one of several coreceptors that are members of the chemokine receptor family (Broder and Dimitrov, 1996; D'Souza and Harden, 1996; Wilkinson, 1996). The membrane-spanning gp41 subunit then promotes fusion of the viral and cellular membranes, a process that results in the release of viral contents into the host cell.

The HIV envelope glycoprotein complex shares several features with other viral membrane-fusion proteins, including the hemagglutinin (HA) protein of influenza virus, for which the mechanism of membrane fusion has been studied in greater detail (Wiley and Skehel, 1987; Stegmann and Helenius, 1993). For example, HA is proteolytically processed, as is the HIV envelope precursor, to generate a receptor-binding subunit (HA_1) and a membrane-spanning subunit (HA_2) which contains the "fusion" peptide. The hydrophobic fusion-peptide region of HA is known to insert into target membranes as an early event in the membrane fusion process (Stegmann et al., 1991; Tsurudome et al., 1992). In both gp41 and HA_2, the fusion-peptide region begins immediately at the new amino terminus that results from proteolytic processing reviews, (Wiley and Skehel, 1987; Hunter and Swanstrom, 1990; White, 1992). In several viral membrane-fusion proteins, including gp41 and HA_2, the region following the fusion peptide has a high α-helical propensity and a 4-3 heptad repeat of hydrophobic residues, a sequence feature characteristic of coiled coils (Chambers et al., 1990; Delwart et al., 1990; Gallaher et al., 1989). X-ray crystallographic studies of fragments of HA_2 and the transmembrane (TM) subunit of Moloney murine leukemia virus (Mo-MLV) demonstrate that these heptad-repeat regions do form coiled coils, in both cases as homotrimers (Bullough et al., 1994; Fass et al., 1996).

Numerous studies have led to the proposal that there are native (nonfusogenic) and fusion-active (fusogenic) states of viral membrane fusion proteins. In the native HA_1/HA_2 influenza complex, for example, part of the heptad-repeat region of HA_2 folds as a nonhelical loop (Wilson et al., 1981) but converts to a coiled coil when exposed to low pH (Bullough et al., 1994). Since low pH also activates influenza membrane fusion, this conformation of HA is generally regarded to be fusogenic, and we will refer to it as such. The loop to coiled-coil transition is the basis of the "spring-loaded" mechanism for activation of membrane fusion (Carr and Kim, 1993).

Extensive conformational changes in the HIV envelope complex are also thought to be involved in the transition from the native to the fusogenic state. Binding of CD4 to gp120 exposes the V3 loop of gp120, which likely interacts with the coreceptors (Choe et al., 1996; Trkola et al., 1996; Wu et al., 1996). For some laboratory-adapted isolates of HIV-1, the conformational changes in gp120 upon CD4 binding are sufficient to cause gp120 to physically dissociate or "shed" from the viral surface, leaving the membrane-anchored gp41 subunit behind (Moore et al., 1990; Hart et al., 1991). Primary isolates of the virus generally do not shed gp120 readily in the presence of CD4 alone, although CD4 binding still induces conformational changes in gp120 (Sattentau and Moore, 1993; Sattentau et al., 1993; Sullivan et al., 1995; Stamatatos and Cheng-Mayer, 1995). CD4 binding also induces conformational changes in gp41, as inferred from changes in antibody binding and sensitivity to limited proteolysis (Sattentau and Moore, 1991, 1993). Moreover, addition of low levels of soluble CD4 enhances the infectivity of some viral isolates, suggesting that the gp120/gp41 conformational changes induced by CD4 play a role in membrane fusion (Allan et al., 1990; Sullivan et al., 1995). These conformational changes are thought to expose the hydrophobic, glycine-rich fusion-peptide region of gp41 that is essential for membrane-fusion activity.

It has not yet been possible to obtain a detailed structure for gp41, either alone or in complex with gp120. We have therefore applied a protein-dissection approach, in which key substructures of a protein are identified and studied (e.g., Oas and Kim, 1988). Protein dissection has been used successfully to study other viral membrane fusion proteins (Carr and Kim, 1993; Bullough et al., 1994; Fass and Kim, 1995; Fass et al., 1996). Limited proteolysis of a fragment corresponding to the ectodomain of gp41 generated a stable, soluble complex composed of two peptide fragments denoted N51 and C43 (Figure 1) that are derived from the N- and C-terminal regions of the ectodomain, respectively (Lu et al., 1995). The N51 peptide corresponds to the 4-3 hydrophobic repeat region adjacent to the fusion peptide, while the C43 peptide is derived from the region prior to the transmembrane segment (Figure 1).

Interestingly, isolated peptides that overlap, or are derived from, the N51 and C43 regions of gp41 can have potent anti-viral activity (Wild et al., 1992, 1994b; Jiang et al., 1993). Peptides from the C-terminal region of the ectodomain have the highest activity. Consistent with these studies, both N51 and C43 are capable of inhibiting HIV envelope–mediated cell fusion; the C43 peptide exhibits 10-fold greater activity than N51 (Lu et al., 1995). The inhibitory activity of the C43 peptide, however, is markedly reduced when stoichiometric amounts of N51 are present, suggesting that the C43 peptide inhibits membrane fusion in a dominant-negative manner, by associating with an N51 region within intact gp41 (Lu et al., 1995). Thus, in addition to providing insights into the mechanism of membrane fusion, determining the structural basis for interaction between the N51 and C43 regions could assist anti-viral drug-development efforts.

Biophysical studies showed that the N51 and C43 peptides associate to form a highly thermostable, helical, trimeric complex of heterodimers, in which the N51 and C43 helices are oriented in an antiparallel manner (Lu et al., 1995). Analogous experiments with the gp41 ectodomain from simian immunodeficiency virus (SIV) gave almost identical results, indicating that the gp41 core identified in these protein-dissection studies is conserved among lentiviruses (Blacklow et al., 1995). On the basis of these results and other considerations, we proposed that the gp41 core consists of an interior coiled-coil trimer formed by the N51 region, against which three C43 helices pack (Blacklow et al., 1995; Lu et al., 1995).

The thermal denaturation of the N51/C43 complexes from HIV-1 or SIV gp41 are irreversible, probably as a result of aggregation of the unfolded peptides at high temperature (Lu et al., 1995; Blacklow et al., 1995). With a view toward crystallographic studies, further protein dissection experiments were used to define a slightly smaller subdomain with more favorable thermodynamic properties. These studies (M. Lu and P. S. K., unpublished data) led to the identification of the peptides N36 and C34 (Figure 1). Like the longer peptides, N36 and C34 form a stable, trimeric complex of heterodimers with 100% helix content. Unlike the larger complex, however, the N36/C34 complex has a reversible thermal unfolding transition (M. Lu and P. S. K., unpublished data). Here we present the crystal structure of this complex solved to 2.0 Å resolution and discuss the implications of this structure for HIV viral membrane fusion and its inhibition.

Results

Crystals of N36/C34 were grown by sitting-drop vapor diffusion (see Experimental Procedures). An initial model of the complex was built into an electron density map generated by multiwavelength anomalous dispersion (MAD) analysis (review, Hendrickson, 1991) of an osmium-derivatized crystal. Details of data collection and MAD phasing statistics are listed in Table 1. A representative portion of the solvent-flattened electron density map used for building the initial model is shown in Figure 2. The structure was refined against data to 2.0 Å from a native crystal to yield an R_{free} of 0.266 and an R_{cryst} of 0.238 (Table 1).

Structure of the N36/C34 Complex

The N36/C34 complex is a six-stranded helical bundle (Figure 3). The center of this bundle consists of a parallel, trimeric coiled coil of three N36 helices wrapped in a gradual left-handed superhelix. Three C34 helices wrap antiparallel to the N36 helices in a left-handed direction around the outside of the central coiled-coil trimer. This arrangement of helices was anticipated on the basis of sequence analysis and biophysical studies (Lu et al., 1995; Blacklow et al., 1995). The overall dimensions of this complex comprise a cylinder measuring ~35 Å in diameter and ~55 Å in height.

As in other naturally occurring coiled coils (Cohen and Parry, 1990), the interior residues at the **a** and **d** positions of the N36 heptad repeat are predominantly hydrophobic, although occasional buried polar interactions are also present in the central three-stranded coiled coil (Figure 4). A sequence comparison of HIV-1 (HXB2 strain) and SIV (Mac239 strain) gp41 shows that the residues at these two heptad-repeat positions are highly

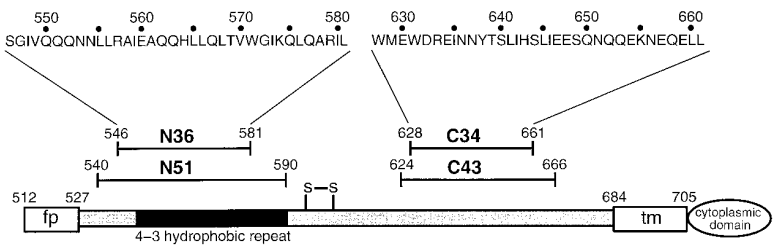

Figure 1. Interacting Peptides Identified in HIV gp41

A schematic view of gp41 showing important functional regions, including the 4-3 hydrophobic repeat, the fusion peptide (fp), a disulfide linkage (S-S), and the transmembrane region (tm). The ectodomain is drawn approximately to scale. The peptides identified by protein dissection are shown above, along with the sequences of N36 and C34. The residues are numbered according to their position in gp160.

Table 1. Crystallographic and Refinement Statistics

Data Collection

Crystal	λ (Å)	Complete (%)	R_{sym}[a] (%)	Resol. (Å)
Native	1.5418	96.5	5.5	2.0
OsO_4 λ1	1.1398	96.4	4.3	2.7
OsO_4 λ2	1.1396	96.4	4.3	2.7
OsO_4 λ3	1.1344	96.8	4.5	2.7
OsO_4 λ4	1.1406	93.4	4.5	2.7

Phasing Statistics[h] (12–2.7 Å)

Derivative	R_{iso}[b] (%)	R_{diff}[c] (%) (weighted)	R_{cullis}[d] Acentric	R_{cullis}[d] Centric	R_{cullis}[d] Anom.	Ph. power[e] Acentric	Ph. power[e] Centric	Occ.[f]	Anom. Occ.[f]
OsO_4 λ1 vs. λ4	4.4	6.7	0.46	0.53	0.21	2.46	1.53	0.075	2.165
OsO_4 λ2 vs. λ4	6.6	9.3	0.37	0.37	0.22	3.34	2.36	0.132	1.784
OsO_4 λ3 vs. λ4	5.4	7.4	0.42	0.44	0.35	2.94	2.12	0.105	1.005

Refinement Statistics (12–2.0 Å)

Nonhydrogen Protein Atoms	Waters	Number of Reflections		R_{cryst}[g]	R_{free}[g]	rms Deviations	
		Working	Free			Bonds (Å)	Angles (°)
596	43	5212	371 (7.12%)	0.238	0.266	0.014	2.742

[a] $R_{sym} = \Sigma\Sigma_j|I_j - \langle I\rangle| / \Sigma|\langle I\rangle|$, where I_j is the recorded intensity of the reflection j and $\langle I\rangle$ is the mean recorded intensity over multiple recordings.

[b] $R_{iso} = \Sigma||F_{(\lambda i)} \pm F_{(\lambda 4)}| - |F_{(\lambda i)}|| / \Sigma|F_{(\lambda 4)}|$, where $F_{(\lambda i)}$ is the structure factor at wavelength λi and $F_{(\lambda 4)}$ is the structure factor at the reference wavelength λ4.

[c] $R_{diff} = [\Sigma|(F^2_{(\lambda 4)} - \Phi_{mean}) / \varphi F^2_{(\lambda 4)}| + |(F^2_{(\lambda i)} - \Phi_{mean}) / \varphi F^2_{(\lambda i)}|] / [\Sigma[(F^2_{(\lambda 4)} / \varphi F^2_{(\lambda 4)}) + (F^2_{(\lambda i)} / \varphi F^2_{(\lambda i)})]]$, where $\Phi_{mean} = [(F^2_{(\lambda 4)} / \varphi F^2_{(\lambda 4)}) + (F^2_{(\lambda i)} / \varphi F^2_{(\lambda i)})] / [(1/\varphi F^2_{(\lambda 4)}) + (1/\varphi F^2_{(\lambda i)})]$ and $\varphi F^2_{(n)} = [\text{Variance } (F^2_{(n)})]4F^2_{(n)}$.

[d] $R_{cullis} = \Sigma||F_{(\lambda i)} \pm F_{(\lambda 4)}| - |F_{h(\lambda i),c}||/\Sigma|F_{(\lambda i)} \pm F_{(\lambda 4)}|$, where $F_{h(\lambda i),c}$ is the calculated heavy atom structure factor.

[e] Phase power = $\langle F_{h(\lambda i)}\rangle$ / E, where $\langle F_{h(\lambda i)}\rangle$ is the root-mean-sqaure heavy atom structure factor and E is the residual lack of closure error.

[f] Occupancies are values output from MLPHARE.

[g] $R_{cryst,\ free} = \Sigma||F_{obs}| - |F_{calc}|| / |F_{obs}|$, where the crystallographic and free R factors are calculated using the working and free reflection sets, respectively.

[h] Overall figure of merit (before solvent flattening): 0.89.

conserved (Figure 4). The characteristic "knobs-into-holes" packing of coiled coils is utilized, whereby the residues (knobs) at the **a** and **d** layers pack into cavities (holes) between four residues of an adjacent helix (Crick, 1953; O'Shea et al., 1991). Of the three types of knobs-into-holes packing geometry observed in coiled-coil structures (Harbury et al., 1993, 1994), the N36 trimer demonstrates exclusively "acute" packing geometry (data not shown), similar to that found in the crystal structure of an isoleucine-zipper trimer (Harbury et al., 1994). This type of packing arrangement in the interior of the coiled coil is characteristic of trimers because it allows β-branched residues (e.g., isoleucine) to pack favorably at both the **a** and **d** positions (Harbury et al., 1994). Trimeric coiled coils, like the N36 trimer (Figure 4), tend to have β-branched residues at both the **a** and **d** positions.

Although complexes of the N and C peptides are clearly trimeric (Lu et al., 1995; Blacklow et al., 1995) isolated N peptides corresponding to the 4-3 hydrophobic repeat from gp41 have been reported to form tetramers, leading to conflicting conclusions regarding the oligomeric state of gp41 (Rabenstein and Shin, 1995, 1996; Lawless et al., 1996; Shugars et al., 1996). An electrostatic potential map of the N36 coiled-coil trimer shows that its surface is largely uncharged (Figure 5). The grooves that are the sites for C34 interaction are lined with predominantly hydrophobic residues (see below) that would be expected to lead to aggregation upon exposure to solvent. Indeed, previous studies have shown that the isolated N-peptides tend to aggregate (Blacklow et al., 1995; Lu et al., 1995). Thus, conclusions regarding the oligomerization state of gp41 based on studies of isolated N-peptides are probably misleading. The N36/C34 complex shows a much more highly charged surface due to acidic residues on the outside of the C34 helices (Figure 5), explaining the greater solubility of the heterodimeric complex.

Interactions between the N and C Peptide Helices

Three C34 helices pack obliquely against the outside of the N36 coiled-coil trimer in an antiparallel orientation. These C34 helices interact with N36 mainly through hydrophobic residues in three grooves on the surface of the central coiled-coil trimer. Sequence comparisons between HIV and SIV gp41 show that the residues lining these grooves are highly conserved (Figure 6). In contrast, the N36 residues flanking the C34 helices are divergent between HIV and SIV (Figure 6).

This pattern of sequence conservation is also apparent on a helical wheel representation of three N36 helices and one C34 helix (Figure 4). In this diagram, the residue positions in C34 are depicted as ellipses to indicate the oblique tilt of the C34 helix relative to the N36 superhelix and to emphasize that C34 is not part of a coiled coil. Residues at the **e** and **g** positions of the N36 helices lie on the outside of the central coiled coil and point into the triangular interhelical space between two N36 helices and a buttressing C34 helix. In general, residues at positions **a** and **d** of C34 pack against residues at the

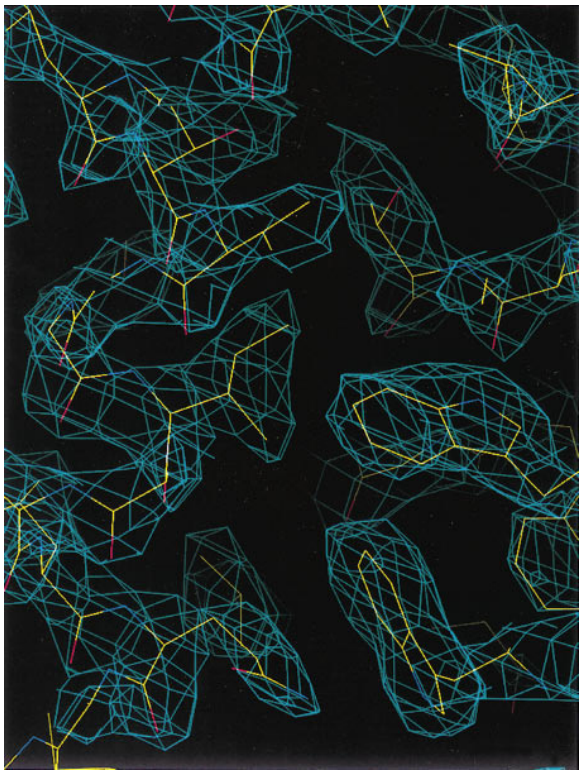

Figure 2. Experimental Electron Density Map

A representative portion of the initial electron density map calculated using experimental structure-factor amplitudes and solvent-flattened MAD phases is shown with the refined molecular model. The map is contoured at 1.5 standard deviations above the mean density. The figure was generated with the program O (Jones and Kjeldgaard, 1992).

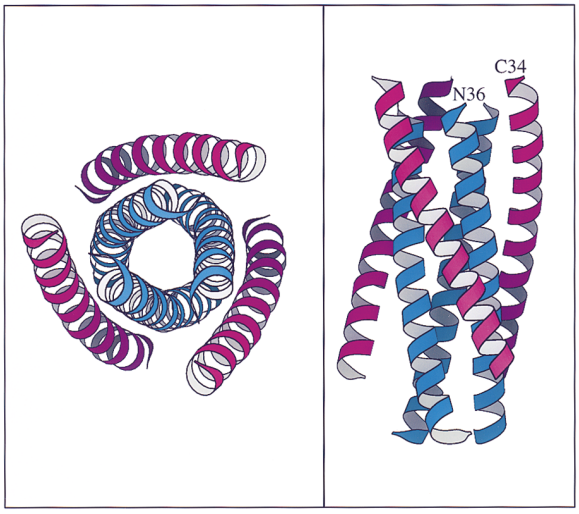

Figure 3. Overall Views of the N36/C34 Complex

The left panel shows an end-on view of the N36/C34 complex looking down the three-fold axis of the trimer. The right panel shows a side view with one N36 and one C34 helix labeled. The amino termini of the N36 helices (blue) point toward the top of the page, while those of the C34 helices (purple) point toward the bottom. Diagrams were prepared using the program MOLSCRIPT (Kraulis, 1991).

e and **g** positions of the N36 helices (Figure 4), although contacts at other positions are often observed. Comparing HIV and SIV gp41, no nonconservative changes exist at the **e** and **g** positions of the N36 helix, and only two such changes occur at the **a** and **d** positions of C34. In contrast, 8 of the 9 nonconservative changes in the N36 helix occur at the outside **f**, **b**, and **c** positions, while 13 of the 15 nonconservative changes in the C34 helix occur at positions other than **a** and **d**. The sequence of the N-peptide region of gp41 is among the most highly conserved within the HIV envelope glycoprotein. Our results show that the high sequence conservation in this region results from selective pressure on the **e** and **g** positions to retain C34 peptide interactions, as well as pressure on the **a** and **d** positions to maintain trimeric coiled-coil interactions.

Each of the grooves on the surface of the N36 trimer has a particularly deep cavity (Figure 7, left panel). This cavity is large (~16 Å long, ~7 Å wide, and 5–6 Å deep) and accommodates three hydrophobic residues from the abutting C34 helix: Ile-635, Trp-631, and Trp-628. As depicted in Figure 7 (right panel), the top of the cavity is lined by Leu-566 of the left N36 helix and Leu-565 of the right N36 helix. Side chains from the left N36 helix form the left side of the cavity, including residues (top to bottom) Val-570, Lys-574 (aliphatic portion), and Gln-577. The right wall is formed by residues Leu-568, Trp-571, and Gly-572 of the right N36 helix. The floor of the cavity is composed of Thr-569, Ile-573, and Leu-576. With the exception of Ile-573 (which is replaced by Thr), all the residues forming the cavity are identical between HIV-1 and SIV. In addition to these predominately hydrophobic interactions within the cavity, Asp-632 of C34 forms a conserved salt bridge with Lys-574 of N36 immediately to the left of the cavity.

Similarity to the Low-pH-Induced Conformation of HA

The N36/C34 complex shows striking structural similarity to the low-pH-induced conformation of the influenza HA_2 subunit ($TBHA_2$) (Bullough et al., 1994) and to the TM subunit of Mo-MLV (Fass et al., 1996), each of which has been proposed to be a fusogenic conformation. Remarkably, the core of each of the three structures contains a three-stranded coiled coil that would be adjacent to the amino-terminal fusion peptide (Figure 8). The trimeric coiled coil of gp41 is very similar to that of the Mo-MLV TM, both having a similar superhelical pitch (~175 Å) and a regular 4-3 periodicity. In contrast, the $TBHA_2$ coiled coil is atypical because it contains two regions with skips in the 4-3 periodicity, resulting in an underwound superhelix (pitch of 300–400 Å). As in the gp41 core structure, $TBHA_2$ contains three antiparallel helices that are packed, with a left-handed tilt, against the central trimeric coiled coil.

Discussion

Evidence That the N36/C34 Structure Corresponds to the Core of the Fusion-Active Conformation

The structure obtained in these studies could, in principle, correspond to the core of gp41 in either the fusogenic or the native state of the envelope glycoprotein, or both. Several considerations provide good evidence

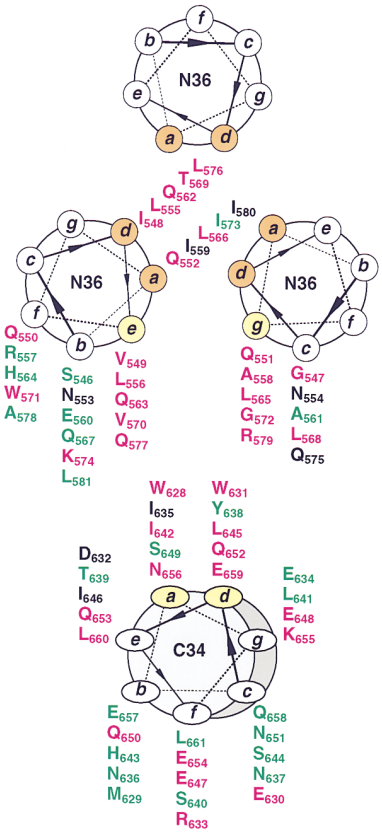

Figure 4. Helical Wheel Representation of N36 and C34

Three N36 helices and one C34 helix are represented as helical wheel projections. The view is from the top of the complex, as in the left panel of Figure 3. The residues at each position are colored according to their conservation between HIV-1 (HXB2) and SIV (Mac239): red, identity; black, conservative change; green, nonconservative change. The N36 helices interact through "knobs-into-holes" packing interactions at the **a** and **d** positions (colored orange). Positions of the N36 and C34 helices that occupy the interhelical space between two N36 helices and a C34 helix are shown in yellow. The helical wheel positions in C34 are indicated by ellipses to represent the oblique orientation of this helix relative to N36. At the top of the complex, C34 is slightly tilted toward the left N36 helix, while at the bottom of the complex (indicated by darker shading), it is slightly tilted toward the right N36 helix.

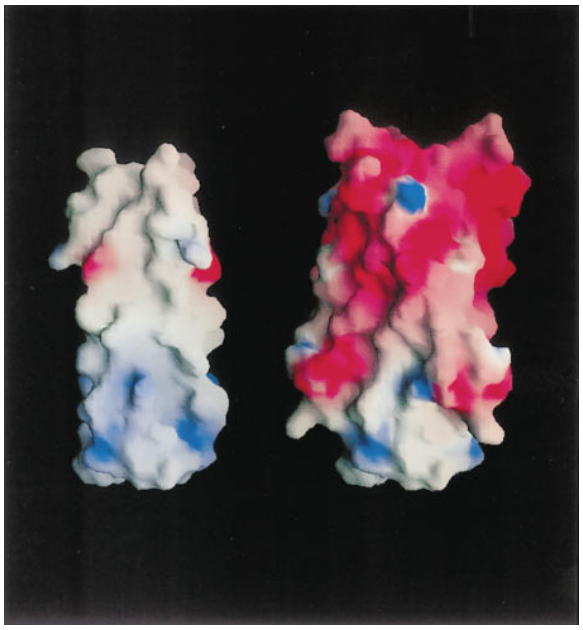

Figure 5. Electrostatic Potential Maps of the Trimer and N36/C34 Complex

An electrostatic potential map (± 7 k_BT/e, where k_B = Boltzmann's constant and T = absolute temperature) of the N36 trimer (left) and N36/C34 complex (right). Regions of basic potential are colored blue, while acidic regions are red. Figure was created with the program GRASP (Nicholls et al., 1991).

that this conformation of gp41 is found in the fusion-active state of HIV envelope.

First, the N36/C34 complex folds in the absence of gp120. The fusogenic state of gp41 is expected to be stable in the absence of gp120, since dissociation of gp120 from the envelope glycoprotein is thought to accompany the conversion from a native to a fusogenic state (Cohen, 1996; Wilkinson, 1996). Similarly, the conversion of influenza HA_2 to the fusogenic state is accompanied by loss of most of its contacts with HA_1. Proteolysis of the low-pH-converted form of HA prior to crystallization removes most of the receptor-binding HA_1 subunit (Bullough et al., 1994). Moreover, the structural features of the fusogenic state are preserved in fragments of HA_2 that fold cooperatively in the complete absence of the HA_1 subunit (Carr and Kim, 1993; Chen et al., 1995b).

Second, the isolated gp41 core is exceedingly stable to thermal denaturation. The N51/C43 complex has an apparent melting temperature of approximately 90°C (Lu et al., 1995). In contrast, the native state of the HIV envelope glycoprotein is not particularly stable, as evidenced by the ease with which gp120 is shed in preparations of virus particles (Kalyanaraman et al., 1990; Helseth et al., 1991).

Third, mutations in gp41 that abolish infectivity and membrane fusion often map to residues that are expected to stabilize the gp41 core structure determined here. Numerous studies show that mutations in the 4-3 hydrophobic repeat region abolish membrane fusion, although these mutants tend to have additional defects (Dubay et al., 1992; Chen et al., 1993; Chen, 1994; Wild et al., 1994a; Poumbourios et al., 1997). The Leu-568→Ala, Trp-571→Arg, and Asn-656→Leu mutations are particularly noteworthy because cells expressing mutant envelope glycoproteins with one of these point mutations are completely defective in membrane fusion, as judged by an inability to form syncytia with CD4-positive human lymphocyte lines, even though the mutant proteins exhibit substantial cell-surface expression, CD4 binding, gp120/gp41 association, gp160 precursor processing, and soluble CD4-induced shedding (Cao et al., 1993). Leu-568 and Trp-571 are N36 residues that line the right wall of the cavity shown in Figure 7 (right panel). Asn-656 is in an **a** position of the C34 peptide and packs against the central N36 coiled-coil trimer. The locations of these key mutations suggest that interactions between the N36 and C34 helices are critical for membrane fusion.

Fourth, our proposal that the N36/34 structure corresponds to the core of the fusogenic state of gp41 is

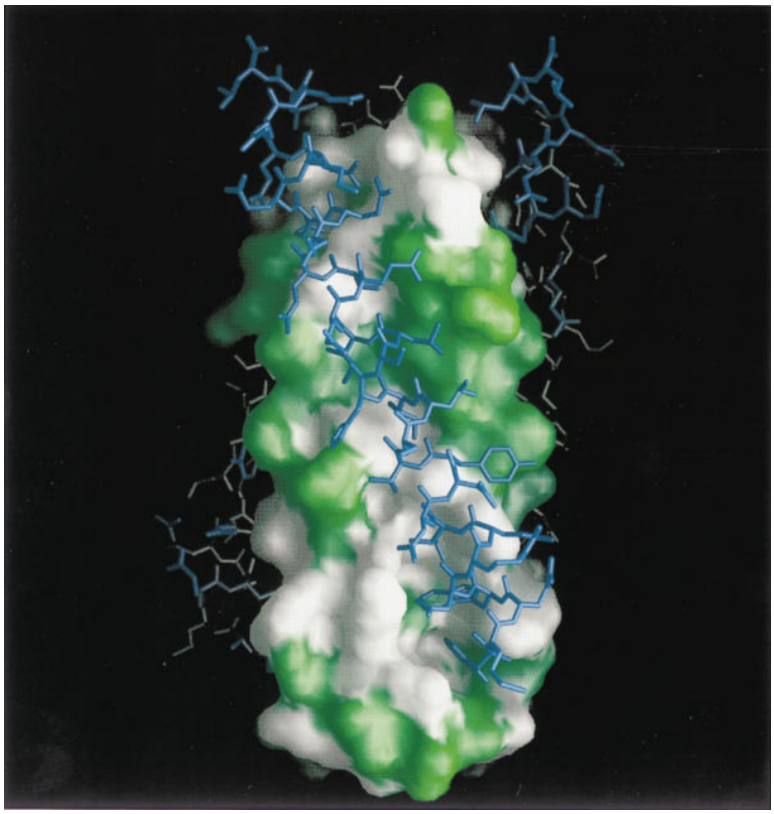

Figure 6. Conserved Grooves on the Surface of the N36 Trimer

The C34 peptides, represented by blue rods, are shown against a surface representation of the N36 trimer. Residues on the surface of the N36 trimer that are identical between HIV and SIV are colored white, and nonidentical residues are green. Note that the C34 helix packs into a conserved (white) groove on the surface of the trimer, while nonconserved (green) regions of N36 are mostly surface-exposed.

consistent with a large body of data on the inhibition of HIV-1 infection and syncytia formation by derivatives of the peptides that make up this core. This issue is discussed in more detail below.

Finally, the structural similarity of the N36/C34 complex to the low-pH-induced conformation of influenza HA_2 (Bullough et al., 1994) and to the structure of Mo-MLV TM (Fass et al., 1996), each of which has been proposed to represent fusion-active conformations, suggests that N36/C34 is the core of the fusogenic conformation of gp41. For all three structures, the hydrophobic fusion peptide would be immediately amino terminal to a central, three-stranded coiled coil. In influenza HA_2 and HIV-1 gp41, the central three-stranded coiled coils are each stabilized by three helices that pack obliquely against the coiled-coil trimer in an antiparallel manner. In the TM subunit of Mo-MLV, these obliquely packed helices are replaced by a short helix and an extended region that serve a similar structural role.

Inhibitors of HIV-1 Infection

Synthetic peptides containing approximately 40 residues from gp41 that overlap, or include all of, the residues in N36 or C34 can be effective inhibitors, at micromolar to nanomolar concentrations, of HIV infection and syncytia formation (Wild et al., 1992, 1994b; Jiang et al., 1993; Lu et al., 1995). Our earlier investigation into the inhibitory properties of the N51 and C43 peptides implied that these peptides work in a dominant-negative manner (Herskowitz, 1987) by binding to viral gp41 (Lu et al., 1995), a conclusion that was also reached through studies of a gp41 ectodomain chimeric protein (Chen et al., 1995a). Further evidence in support of a dominant-negative mechanism is provided by the finding that mutations in C-peptide derivatives that disrupt their interactions with N peptide correlate with decreased potency as inhibitors (Wild et al., 1995).

The gp41 core crystal structure is fully consistent with this dominant-negative mechanism of inhibition (Figures 3 and 6). The C-peptide derivatives could act as dominant-negative inhibitors by binding to the endogenous N-peptide coiled-coil trimer within viral gp41. The N peptides might inhibit fusion by interfering with formation of the central, coiled-coil trimer within viral gp41 and/or by binding to endogenous viral C-peptide regions.

Both the N- and C-peptide classes of inhibitors are effective against a wide range of HIV strains, including laboratory-adapted strains and primary isolates (Wild et al., 1992; Jiang et al., 1993; Wild et al., 1994b). In contrast, soluble CD4 and many neutralizing antibodies are typically effective only on a limited subset of HIV strains (e.g., Nara et al., 1988; Palker et al., 1988; Daar et al., 1990; Moore et al., 1995). There is a striking conservation of residues involved in interactions between the N peptide and C peptide, comparing gp41 from HIV-1 and SIV (Figure 6). We conclude that the broad neutralizing effects of the N and C peptides derive from the strong sequence conservation of these residues.

The highly conserved, deep cavities on the N-peptide coiled-coil trimer that accommodate conserved C-peptide residues are attractive targets for the development of new peptidomimetic or small-molecule inhibitors of HIV infection. The two indole rings and neighboring side chains that occupy the prominent cavity depicted in

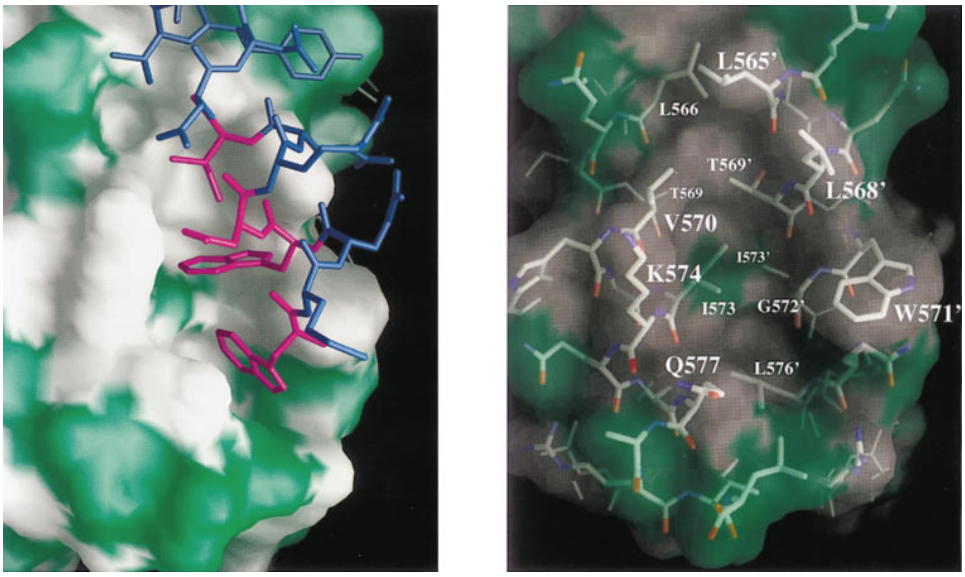

Figure 7. Interaction of C34 Residues with a Large Cavity on the N36 Trimer Surface

(Left panel) A surface representation of the cavity in the carboxy-terminal portion of the N36 trimer, colored as in Figure 6. Residues in C34 that dock into this pocket are colored purple (Ile-635, Asp-632, Trp-631, and Trp-628). (Right panel) Residues that form the cavity in the N36 coiled-coil surface are labeled. A prime (′) is used to distinguish residues of one N36 helix from those of an adjacent N36 helix. This orientation is rotated ~30° to the left relative to the left panel, in order to facilitate visualization of all the side chains.

Figure 7 are a particularly attractive starting point for the design and/or development of new drugs. Not only is this cavity deep and highly conserved, but two of the three key mutations that disrupt membrane fusion, discussed above, map to one wall of this cavity (Figure 7). Because some of the known potent peptide inhibitors (Wild et al., 1994b) extend beyond N36 and C34 and do not involve this cavity region, it is likely that other distinctive surface features exist in the interface between the N and C helices of longer peptides such as N51 and C43 (Lu et al., 1995). The importance of identifying drugs that target the HIV membrane-fusion machinery is emphasized by the success of combination drug regimens for the treatment of AIDS (review, Lipsky, 1996). As yet, these combination therapies do not target the HIV envelope.

Implications for gp41 Function and Viral Membrane Fusion

The structures of the cores of the membrane-fusion subunits from HIV, Mo-MLV, and influenza virus are remarkably similar (Figure 8). It appears that these diverse viruses present fusion peptides to target cells via a common scaffold, in which the fusion peptides are atop a central, three-stranded coiled coil that is supported by additional, carboxy-terminal structures. This scaffold is likely to be a common feature of viral membrane-fusion proteins since many of these proteins contain coiled-coil signature sequences, with 4-3 heptad repeats of hydrophobic amino acids, adjacent to an amino-terminal fusion-peptide region (Gallaher et al., 1989; Chambers et al., 1990; Delwart et al., 1990). Moreover, studies of the fusion proteins of several paramyoviruses have identified regions with similarity to the N- and C-peptide regions of HIV and SIV gp41 (Lambert et al., 1996). These common structural features suggest that the rich body of work investigating the mechanism of membrane fusion for many other viruses, including influenza, is relevant for understanding the mechanism of HIV-mediated membrane fusion.

Given the similarity in structure between the HIV gp41 core and the low-pH-converted conformation of HA_2, it is worth considering whether the structural rearrangements that occur during the transition of HA_2 to the fusogenic state are analogous to those in gp41. In the native, nonfusogenic conformation of influenza HA, part of the N-terminal coiled-coil trimer seen in the fusogenic state (Bullough et al., 1994) is held in a nonhelical, hairpin structure, as a result of extensive interactions with the receptor-binding HA_1 subunit (Wilson et al., 1981). Thus, the receptor-binding HA_1 subunit acts as a "clamp" that binds this N-terminal region of HA_2, holding it in the non-coiled-coil conformation. The receptor-binding domains dissociate in the fusogenic conformation of HA, as in HIV, although in the case of influenza, the HA_1 subunits are still tethered via a disulfide bond to HA_2. Upon release of the HA_1 clamp, a dramatic conformational change in HA_2 occurs, including coiled-coil formation by this N-terminal region (Carr and Kim, 1993; Bullough et al., 1994).

A substantial conformational change in the envelope glycoprotein complex is also thought to be critical during HIV infection, though few details are understood. It remains to be determined whether the HIV envelope complex also utilizes coiled-coil formation as part of a spring-loaded mechanism, or if the gp41 core structure determined here is present in the native as well as the fusogenic state. It is possible that the N36/C34 structure is the core structure of gp41 even when it is bound to gp120, and that release of gp120 simply exposes the

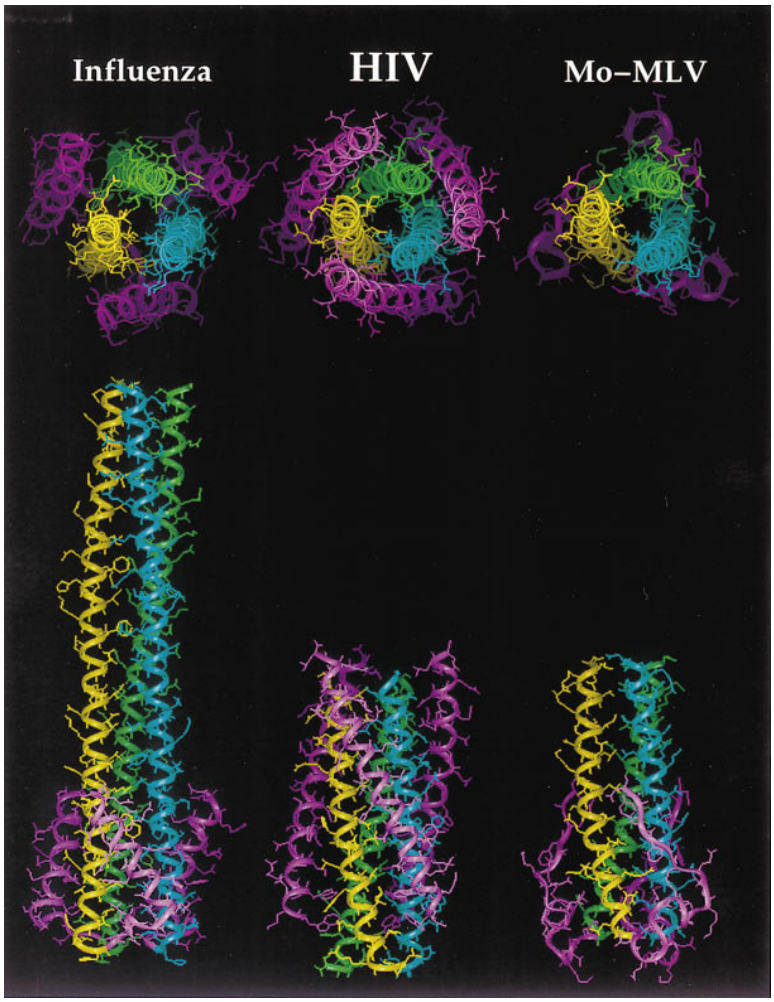

Figure 8. Comparison of Influenza HA_2, HIV gp41, and Mo-MLV TM Structures

The top panel shows an end-on view of the three structures from the top, as in the left panel of Figure 3. The bottom panel shows a side view. The three monomers forming the central coiled coil of each structure are colored yellow, green, and blue. Supporting structures are colored purple. Residues 40–129 of HA_2 (Bullough et al., 1994) and 45–98 of Mo-MLV TM (Fass et al., 1996) are included. The figure was generated using the program Insight (Biosym).

fusion-peptide region of gp41. Alternatively, HIV gp120, like influenza HA_1, may serve as a clamp that represses formation of the N36/C34 structure presented here, with gp120 shedding allowing its formation. This gp41 core structure serves as the starting point for addressing this and other essential structural questions about the mechanism of HIV entry into cells.

Experimental Procedures

Peptide Purification and Crystallization

Peptides N36 and C34 were synthesized by standard FMOC peptide chemistry and have an acetylated N terminus and a C-terminal amide. N36 corresponds to residues 546–581 of gp160, while C34 corresponds to residues 628–661. After cleavage from the resin, the peptides were desalted on a Sephadex G-25 column (Pharmacia) and lyophilized. Peptides were then purified by reverse-phase high performance liquid chromatography (Waters, Inc.) on a Vydac C18 preparative column. The identity of the peptides was verified by mass spectrometry. Peptide concentration was determined by tyrosine and tryptophan absorbance in 6 M GuHCl (Edelhoch, 1967).

To grow crystals, a 10 mg/ml stock of the N36/C34 complex was diluted 1:1 in a sitting drop with 80 mM NH_4Cl, 20% PEG200, and 50% isopropanol and allowed to equilibrate against a reservoir of 80 mM NH_4Cl, 20% PEG200, and 30% isopropanol. Crystals grew as hexagonal prisms and belonged to the space group P321 ($a = b = 49.5$ Å, $c = 55.3$ Å). For native data sets and heavy atom screens, crystals were flash-frozen in a MSC cryogenic crystal cooler (X-stream), and data was collected on a Rigaku RU-200 rotating-anode X-ray generator with an R-axis IIc detector.

Heavy Atom Screen and Phase Determination

Multiwavelength anomalous diffraction (MAD) data were collected at the Howard Hughes Medical Institute beamline X4A of the National Synchrotron Light Source at Brookhaven National Laboratory. Fluorescence spectra (1.1459–1.1354 Å) were obtained from a single flash-frozen crystal soaked in 0.04% OsO_4 in harvest buffer (80 mM NH_4Cl, 20% PEG200, 30% isopropanol) for 4 hr. Based on the fluorescence profile, individual data sets were collected on Fuji imaging plates at four wavelengths ($\lambda_1 = 1.1396$ Å, $\lambda_2 = 1.1398$ Å, $\lambda_3 = 1.1402$ Å, and $\lambda_4 = 1.1344$ Å). Reflections were integrated and scaled with DENZO and SCALEPACK (Otwinowski, 1993).

Data scaling, phase determination, and map generation were all performed using the CCP4 suite of programs (CCP4, 1994). Anomalous and dispersive difference Patterson maps from MAD data sets all showed a single clear peak corresponding to the osmium binding site. The position of the site was calculated from the single $z = 0$ Harker section and from cross-peaks found at $z = 0.28$ and $z = 0.71$. Phases generated with the program MLPHARE (Otwinowski, 1991) gave an overall figure of merit of 0.89 (Table 1) and produced an interpretable electron density map with a clear solvent boundary. Density modification was subsequently performed using DM (Cowtan, 1994), resulting in maps of high quality in which electron density for the entire main chain and all side chains was evident (Figure 2).

Model Refinement

The polypeptide chain was traced and the side chains readily positioned into a 2.7 Å density-modified map using the program O (Jones

and Kjeldgaard, 1992). The initial model of N36/C34 was refined with the program XPLOR (Brünger, 1992a) against data to 2.0 Å from a native crystal. An anisotropic B-factor was applied to the native structure factors using XPLOR, and a free R set (Brünger, 1992b) was taken from the data prior to refinement (Table 1). The model was refined by iterative cycles of grouped B-factor, positional, and individual B-factor refinement. As the refinement proceeded, 43 waters were added and a bulk solvent correction was applied. At no time during the refinement did the molecule differ enough from the original model so as to require manual rebuilding, though main chain and side chain geometries were optimized in O between cycles of refinement. The quality of the structure was verified by PROCHECK (Laskowski et al., 1993), with all residues but one (Ile-580) occupying most-preferred regions of Ramachandran space. Ile-580 lies in the additionally allowed region of Ramachandran space and is the second residue from the C terminus of the N36 peptide; inspection of the solvent-flattened MAD-phased maps confirmed its position. Refined coordinates will be deposited in the Protein Data Bank (Brookhaven National Laboratory, Upton, NY).

Acknowledgments

We thank the staff, particularly Dr. Craig Ogata, of the Howard Hughes Medical Institute beamline (X4A) at the National Synchrotron Light Source at Brookhaven National Laboratory for invaluable support in collecting MAD data. We are also grateful to Debra Ehrgott and Li Su for help with data collection, Michael Burgess and James Pang for peptide synthesis, and Dr. Steven J. Gamblin for helpful suggestions. D. C. C. is supported by a postdoctoral fellowship from the Jane Coffin Childs Memorial Fund for Medical Research. J. M. B. is a Whitehead Fellow and acknowledges support from the W. M. Keck Foundation. This work was funded by the Howard Hughes Medical Institute and utilized the W. M. Keck Foundation X-ray Crystallography Facility at the Whitehead Institute.

Received April 3, 1997; revised April 7, 1997.

References

Allan, J.S., Allan, J.S., Strauss, J., and Buck, D.W. (1990). Enhancement of SIV infection with soluble receptor molecules. Science *247*, 1084–1088.

Blacklow, S.C., Lu, M., and Kim, P.S. (1995). A trimeric subdomain of the simian immunodeficiency virus envelope glycoprotein. Biochemistry *34*, 14955–14962.

Broder, C.C., and Dimitrov, D.S. (1996). HIV and the 7-transmembrane domain receptors. Pathobiology *64*, 171–179.

Brünger, A.T. (1992a). A system for X-ray crystallography and NMR. X-PLOR Version 3.1. (New Haven, Connecticut: Yale University Press).

Brünger, A.T. (1992b). Free R value: a novel statistical quantity for assessing the accuracy of crystal structures. Nature *355*, 472–475.

Bullough, P.A., Hughson, F.M., Skehel, J.J., and Wiley, D.C. (1994). Structure of influenza haemagglutinin at the pH of membrane fusion. Nature *371*, 37–43.

Cao, J., Bergeron, L., Helseth, E., Thali, M., Repke, H., and Sodroski, J. (1993). Effects of amino acid changes in the extracellular domain of the human immunodeficiency virus type 1 gp41 envelope glycoprotein. J. Virol. *67*, 2747–2755.

Carr, C.M., and Kim, P.S. (1993). A spring-loaded mechanism for the conformational change of influenza hemagglutinin. Cell *73*, 823–832.

CCP4 (1994). Collaborative computational project, Number 4. Acta Cryst. *D50*, 760–763.

Chambers, P., Pringle, C.R., and Easton, A.J. (1990). Heptad repeat regions are located adjacent to hydrophobic regions in several types of virus fusion glycoproteins. J. Gen. Virol. *71*, 3075–3080.

Chen, C.H., Matthews, T.J., McDanal, C.B., Bolognesi, D.P., and Greenberg, M.L. (1995a). A molecular clasp in the human immunodeficiency virus (HIV) type 1 TM protein determines the anti-HIV activity of gp41 derivatives: implication for viral fusion. J. Virol. *69*, 3771–3777.

Chen, J., Wharton, S.A., Weissenhorn, W., Calder, L.J., Hughson, F.M., Skehel, J.J., and Wiley, D.C. (1995b). A soluble domain of the membrane-anchoring chain of influenza virus hemagglutinin (HA_2) folds in Escherichia coli into the low-pH-induced conformation. Proc. Natl. Acad. Sci. USA *92*, 12205–12209.

Chen, S.S. (1994). Functional role of the zipper motif region of human immunodeficiency virus type 1 transmembrane protein gp41. J. Virol. *68*, 2002–2010.

Chen, S.S., Lee, C.N., Lee, W.R., McIntosh, K., and Lee, T.H. (1993). Mutational analysis of the leucine zipper-like motif of the human immunodeficiency virus type 1 envelope transmembrane glycoprotein. J. Virol. *67*, 3615–3619.

Choe, H., Farzan, M., Sun, Y., Sullivan, N., Rollins, B., Ponath, P.D., Wu, L., Mackay, C.R., LaRosa, G., Newman, W., Gerard, N., Gerard, C., and Sodroski, J. (1996). The beta-chemokine receptors CCR3 and CCR5 facilitate infection by primary HIV-1 isolates. Cell *85*, 1135–1148.

Cohen, C., and Parry, D.A. (1990). Alpha-helical coiled coils and bundles: how to design an alpha-helical protein. Proteins *7*, 1–15.

Cohen, J. (1996). Investigators detail HIV's fatal handshake. Science *274*, 502.

Cowtan, K.D. (1994). Joint CCP4 and ESF-EACBM. Newslett. Prot. Crystallogr. *31*, 34–38.

Crick, F.H.C. (1953). The packing of α-helices: simple coiled coils. Acta Cryst. *6*, 689–697.

D'Souza, M.P., and Harden, V.A. (1996). Chemokines and HIV-1 second receptors. Nature Med. *2*, 1293–1300.

Daar, E.S., Li, X.L., Moudgil, T., Ho, D.D. (1990). High concentrations of recombinant soluble CD4 are required to neutralize primary human immunodeficiency virus type 1 isolates. Proc. Natl. Acad. Sci. USA *87*, 6574–6578.

Delwart, E.L., Moialos, G., and Gilmore, T. (1990). Retroviral envelope glycoproteins contain a leucine zipper-like repeat. AIDS Res. Hum. Retroviruses *6*, 703–706.

Dubay, J.W., Roberts, S.J., Brody, B., and Hunter, E. (1992). Mutations in the leucine zipper of the human immunodeficiency virus type 1 transmembrane glycoprotein affect fusion and infectivity. J. Virol. *66*, 4748–4756.

Edelhoch, H. (1967). Spectroscopic determination of tryptophan and tyrosine in proteins. Biochemistry *6*, 1948–1954.

Fass, D., and Kim, P.S. (1995). Dissection of a retrovirus envelope protein reveals structural similarity to influenza hemagglutinin. Curr. Biol. *5*, 1377–1383.

Fass, D., Harrison, S.C., and Kim, P.S. (1996). Structure of Moloney murine virus envelope domain at 1.7Å resolution. Nature Struct. Biol. *3*, 465–469.

Freed, E.O., and Martin, M.A. (1995). The role of human immunodeficiency virus type 1 envelope glycoproteins in virus infection. J. Biol. Chem. *270*, 23883–23886.

Gallaher, W.R., Ball, J.M., Garry, R.F., Griffin, M.C., and Montelaro, R.C. (1989). A general model for the transmembrane proteins of HIV and other retroviruses. AIDS Res. Hum. Retroviruses *5*, 431–440.

Harbury, P.B., Zhang, T., Kim, P.S., and Alber, T. (1993). A switch between two-, three-, and four-stranded coiled coils in GCN4 leucine zipper mutants. Science *262*, 1401–1407.

Harbury, P., Kim, P.S., and Alber, T. (1994). Crystal structure of an isoleucine-zipper trimer. Nature *371*, 80–83.

Hart, T.K., Kirsch, R., Ellens, H., Sweet, R.W., Lambert, D.M., Petteway, S.R., Jr., Learly, J., and Bugelski, P.J. (1991). Binding of soluble CD4 proteins to human immunodeficiency virus type 1 and infected cells induces release of envelope glycoprotein gp120. Proc. Natl. Acad. Sci. USA *88*, 2189–2193.

Helseth, E., Olshevsky, U., Furman, U., and Sodroski, J. (1991). Human immunodeficiency virus type 1 glycoprotein regions important for association with the gp41 transmembrane glycoprotein. J. Virol. *65*, 2119–2123.

Hendrickson, W.A. (1991). Determination of macromolecular structures from anomalous diffraction of synchrotron radiation. Science *254*, 51–58.

Herskowitz, I. (1987). Functional inactivation of genes by dominant negative mutations. Nature *329*, 219–222.

Hunter, E., and Swanstrom, R. (1990). Retrovirus envelope glycoproteins. Curr. Top. Microbiol. Immunol. *157*, 187–253.

Jiang, S., Lin, K., Strick, N., and Neurath, A.R. (1993). HIV-1 inhibition by a peptide. Nature *365*, 113.

Jones, T.A., and Kjeldgaard, M. (1992). O—The Manual (Uppsala, Sweden: http://kaktus.kemi.aau.dk).

Kalyanaraman, V.S., Rodriguez, V., Veronese, F., Rahman, R., Lusso, P., DeVico, A.L., Copeland, T., Oroszlan, S., Gallo, R.C., and Sarngadharan, M.G. (1990). Characterization of the secreted, native gp120 and gp160 of the human immunodeficiency virus type 1. AIDS Res. Hum. Retroviruses *6*, 371–380.

Kraulis, P. (1991). MOLSCRIPT: a program to produce both detailed and schematic plots of protein structures. J. Appl. Crystallogr. *24*, 924–950.

Lambert, D.M., Barney, S., Lambert, A.L., Guthrie, K., Medinas, R., Davis, D.E., Bucy, T., Erickson, J., Merutka, G., and Petteway, S.R., Jr. (1996). Peptides from conserved regions of paramyxovirus fusion (F) proteins are potent inhibitors of viral fusion. Proc. Natl. Acad. Sci. USA *93*, 2186–2191.

Laskowski, R.A., MacArthur, M.W., Moss, D.S., and Thornton, J.M. (1993). PROCHECK: a program to check the stereochemical quality of protein structures. J. Appl. Crystallogr. *26*, 283–291.

Lawless, M., Barney, S., Guthrie, K.I., Bucy, T.B., Petteway, S.R., Jr., and Merutka, G. (1996). HIV-1 membrane fusion mechanism: structural studies of the interactions between biologically-active peptides from gp41. Biochemistry *35*, 13697–13708.

Lipsky, J.J. (1996). Antiretroviral drugs for AIDS. Lancet *348*, 800–803.

Lu, M., Blacklow, S.C., and Kim, P.S. (1995). A trimeric structural domain of the HIV-1 transmembrane glycoprotein. Nature Struct. Biol. *2*, 1075–1082.

Luciw, P.A. (1996). Human immunodeficiency viruses and their replication. In Fields Virology, Third Edition, B.N. Fields, D.M. Knipe, P.M. Howley, R.M. Chanock, J.L. Melnick, T.P. Monath, B. Roizman, and S.E. Straus, eds. (Philadelphia: Lippincott-Raven Publishers), pp. 1881–1952.

Moore, J.P., McKeating, J.A., Weiss, R.A., and Sattentau, Q.J. (1990). Dissociation of gp120 from HIV-1 virions induced by soluble CD4. Science *250*, 1139–1142.

Moore, J.P., Cao, Y., Qing, L., Sattentau, Q.J., Pyati, J., Koduri, R., Robinson, J., Barbas, C.F., III, Burton, D.R., and Ho, D.D. (1995). Primary isolates of human immunodeficiency virus type 1 are relatively resistant to neutralization by monoclonal antibodies to gp120, and their neutralization is not predicted by studies with monomeric gp120. J. Virol. *69*, 101–109.

Nara, P.L., Robey, W.G., Pyle, S.W., Hatch, W.C., Dunlop, N.M., Bess, J.W., Jr., Kelliher, J.C., Arthur, L.O., and Fischinger, P.J. (1988). Purified envelope glycoproteins from human immunodeficiency virus type 1 variants induce individual, type-specific neutralizing antibodies. J. Virol. *62*, 2622–2628.

Nicholls, A., Sharp, K.A., and Honig, B. (1991). Protein folding and association: insights from the interfacial and thermodynamic properties of hydrocarbons. Proteins *11*, 281–296.

Oas, T.G., and Kim, P.S. (1988). A peptide model of a protein folding intermediate. Nature *336*, 42–48.

O'Shea, E.K., Klemm, J.D., Kim, P.S., and Alber, T. (1991). X-ray structure of the GCN4 leucine zipper, a two-stranded, parallel coiled coil. Science *254*, 539–544.

Otwinoski, Z. (1991). Maximum likelihood refinement of heavy atom parameters. In Isomorphous Replacement and Anomalous Scattering. W. Wolf, P.R. Evans, and A.G.W. Leslie, eds. (Warrington, England: SERC, Daresbury Laboratory) pp. 80–86.

Otwinoski, Z. (1993). Oscillation data reduction program. In Data Collection and Processing. L. Sawyer, N. Isaacs, S. Bailey, eds. (Warrington, England: SERC, Daresbury Laboratory) pp. 56–62.

Palker, T.J., Clark, M.E., Langlois, A.J., Matthews, T.J., Weinhold, K.J., Randall, R.R., Bolognesi, D.P., and Haynes, B.F. (1988). Type-specific neutralization of the human immunodeficiency virus with antibodies to env-encoded synthetic peptides. Proc. Natl. Acad. Sci. USA *85*, 1932–1936.

Poumbourios, P., Wilson, K.A., Center, R.J., El Ahmar, W., and Kemp, B.E. (1997). Human immunodeficiency virus type 1 envelope glycoprotein oligomerization requires the gp41 amphipathic alpha-helical/leucine zipper-like sequence. J. Virol. *71*, 2041–2049.

Rabenstein, M.D., and Shin, Y.K. (1996). HIV-1 gp41 tertiary structure studied by EPR spectroscopy. Biochemistry *35*, 13922–13928.

Rabenstein, M., and Shin, Y.K. (1995). A peptide from the heptad repeat of human immunodeficiency virus gp41 shows both membrane binding and coiled-coil formation. Biochemistry *34*, 13390–13397.

Sattentau, Q.J., and Moore, J.P. (1991). Conformational changes induced in the human immunodeficiency virus envelope glycoprotein by soluble CD4 binding. J. Exp. Med. *174*, 407–415.

Sattentau, Q.J., and Moore, J.P. (1993). The role of CD4 in HIV binding and entry. Phil. Trans. Royal Soc. B *342*, 59–66.

Sattentau, Q.J., Moore, J.P., Vignaux, F., Traincard, F., and Poignard, P. (1993). Conformational changes induced in the envelope glycoproteins of the human and simian immunodeficiency viruses by soluble receptor binding. J. Virol. *67*, 7383–7393.

Shugars, D.C., Wild, C.T., Greenwell, T.K., and Matthews, T.J. (1996). Biophysical characterization of recombinant proteins expressing the leucine zipper-like domain of the human immunodeficiency virus type 1 transmembrane protein gp41. J. Virol. *70*, 2982–2991.

Stamatatos, L., and Cheng-Mayer, C. (1995). Structural modulations of the envelope gp120 glycoprotein of human immunodeficiency virus type 1 upon oligomerization and differential V3 loop epitope exposure of isolates displaying distinct tropism upon virion-soluble receptor binding. J. Virol. *69*, 6191–6198.

Stegmann, T., Delfino, J.M., Richards, F.M., and Helenius, A. (1991). The HA_2 subunit of influenza hemagglutinin inserts into the target membrane prior to fusion. J. Biol. Chem. *266*, 18404–18410.

Stegmann, T., and Helenius, A. (1993). Influenza virus fusion: from models toward a mechanism. In Viral Fusion Mechanisms, J. Bentz, ed. (Boca Raton, Florida: CRC Press), pp. 89–111.

Sullivan, N., Sun, Y., Li, J., Hofmann, W., and Sodroski, J. (1995). Replicative function and neutralization sensitivity of envelope glycoproteins from primary and T-cell line-passaged human immunodeficiency virus type 1 isolates. J. Virol. *69*, 4413–4422.

Trkola, A., Dragic, T., Arthos, J., Binley, J.M., Olson, W.C., Allaway, G.P., Cheng-Mayer, C., Robinson, J., Maddon, P.J., and Moore, J.P. (1996). CD4-dependent, antibody-sensitive interactions between HIV-1 and its co-receptor CCR-5. Nature *384*, 184–187.

Tsurudome, M., Glück, R., Graf, R., Falchetto, R., Schaller, U., and Brunner, J. (1992). Lipid interactions of the hemagglutinin HA_2 NH2-terminal segment during influenza virus-induced membrane fusion. J. Biol. Chem. *267*, 20225–20232.

White, J.M. (1992). Membrane fusion. Science *258*, 917–924.

Wild, C.T., Oas, T., McDanal, C.B., Bolognesi, D., and Matthews, T.J. (1992). A synthetic peptide inhibitor of human immunodeficiency virus replication: correlation between solution structure and viral inhibition. Proc. Natl. Acad. Sci. USA *89*, 10537–10541.

Wild, C., Dubay, J.W., Greenwell, T., Baird, T., Jr., Oas, T.G., McDanal, C., Hunter, E., and Matthews, T. (1994a). Propensity for a leucine zipper-like domain of human immunodeficiency virus type 1 gp41 to form oligomers correlates with a role in virus-induced fusion rather than assembly of the glycoprotein complex. Proc. Natl. Acad. Sci. USA *91*, 12676–12680.

Wild, C.T., Shugars, D.C., Greenwell, T.K., McDanal, C.B., and Matthews, T.J. (1994b). Peptides corresponding to a predictive α-helical domain of human immunodeficiency virus type 1 gp41 are potent inhibitors of virus infection. Proc. Natl. Acad. Sci. USA *91*, 9770–9774.

Wild, C., Greenwell, T., Shugars, D., Rimsky-Clarke, L., and Matthews, T. (1995). The inhibitory activity of an HIV type 1 peptide correlates with its ability to interact with a leucine zipper structure. AIDS Res. Hum. Retroviruses *11*, 323–325.

Wiley, D.C., and Skehel, J.J. (1987). The structure and function of the hemagglutinin membrane glycoprotein of influenza virus. Annu. Rev. Biochem. *56*, 365–394.

Wilkinson, D. (1996). HIV-1: cofactors provide the entry keys. Curr. Biol. *6*, 1051–1053.

Wilson, I.A., Skehel, J.J., and Wiley, D.C. (1981). Structure of the haemagglutinin membrane glycoprotein of influenza virus at 3 Å resolution. Nature *289*, 366–373.

Wu, L., Gerard, N.P., Wyatt, R., Choe, H., Parolin, C., Ruffing, N., Borsett, A., Cardoso, A.A., Desjardin, E., Newman, W., Gerard, C., and Sodroski, J. (1996). CD4-induced interaction of primary HIV-1 gp120 glycoproteins with the chemokine receptor CCR-5. Nature *384*, 179–183.